AD_____

Award Number: W81XWH-04-1-0836

TITLE: Molecular Profiling of Prostate Cancer to Determine Predictive Markers of Response to Radiation and Receptor Tyrosine Kinase Inhibitor Therapy

PRINCIPAL INVESTIGATOR: Dr. Dong Wook Kim

CONTRACTING ORGANIZATION: Vanderbilt University Medical Center
Nashville TN 37203-6917

REPORT DATE: September 2006

TYPE OF REPORT: Annual Summary

PREPARED FOR: U.S. Army Medical Research and Materiel Command
Fort Detrick, Maryland 21702-5012

REPORT DOCUMENTATION PAGE

Form Approved
OMB No. 0704-0188

1. REPORT DATE *(DD-MM-YYYY)*	**2. REPORT TYPE**	**3. DATES COVERED** *(From - To)*
01-09-2006	Annual Summary	1 Sep 2004 - 31 Aug 2006

4. TITLE AND SUBTITLE
Molecular Profiling of Prostate Cancer to Determine Predictive Markers of Response to Radiation and Receptor Tyrosine Kinase Inhibitor Therapy

5a. CONTRACT NUMBER

5b. GRANT NUMBER
W81XWH-04-1-0836

5c. PROGRAM ELEMENT NUMBER

6. AUTHOR(S)
Dr. Dong Wook Kim

E-Mail: dongnathan@gmail.com

5d. PROJECT NUMBER

5e. TASK NUMBER

5f. WORK UNIT NUMBER

7. PERFORMING ORGANIZATION NAME(S) AND ADDRESS(ES)

Vanderbilt University Medical Center
Nashville TN 37203-6917

8. PERFORMING ORGANIZATION REPORT NUMBER

9. SPONSORING / MONITORING AGENCY NAME(S) AND ADDRESS(ES)
U.S. Army Medical Research and Materiel Command
Fort Detrick, Maryland 21702-5012

10. SPONSOR/MONITOR'S ACRONYM(S)

11. SPONSOR/MONITOR'S REPORT NUMBER(S)

12. DISTRIBUTION / AVAILABILITY STATEMENT
Approved for Public Release; Distribution Unlimited

13. SUPPLEMENTARY NOTES - Original contains colored plates: ALL DTIC reproductions will be in black and white.

14. ABSTRACT

Ionizing radiation(IR)induces the activation of PI3K/Akt signaling pathway, which in turn regulates endothelial cell viability during treatment with radiotherapy. Inhibition of this pathway by receptor tyrosine kinase inhibitor (TKIs) enhances the cytotoxic effects of radiation in tumor vascular endothelium resulting in improved tumor control. There is significant evidence that multiple receptor tyrosinse kinases may be aberrantly activated in the prostate cancer cells. Therefore, we sought to study the effects of broad spectrum small molecule TKIs in the prostate tumor models. We demonstrate that inhibition of this pathway results in improved control of prostate tumor treated with IR via dual effect on both the tumor cells, and its microvasculature. Using innovative proteomic technology, we plan to identify the molecular profiles that are predictive of response to TKI and IR therapy. Our goal is for these results to provide insights in designing clinical studies aimed at taking these promising pipeline compounds to help treat patients with high risk prostate cancer.

15. SUBJECT TERMS
radiation oncology, proteomics, prostate cancer, molecular profiling, receptor tyrosine kinase inhibitors

16. SECURITY CLASSIFICATION OF:			**17. LIMITATION OF ABSTRACT**	**18. NUMBER OF PAGES**	**19a. NAME OF RESPONSIBLE PERSON**
a. REPORT	**b. ABSTRACT**	**c. THIS PAGE**			USAMRMC
U	U	U	UU	30	**19b. TELEPHONE NUMBER** *(include area code)*

Standard Form 298 (Rev. 8-98)
Prescribed by ANSI Std. Z39.18

Introduction:

Our laboratory has previously demonstrated that ionizing radiation (IR) induces the activation of PI3K/Akt, which in turn regulates endothelial cell viability during treatment with radiotherapy. Interestingly, inhibition of this pathway by receptor tyrosine kinase inhibitor (TKIs) enhances the cytotoxic effects of radiation in tumor vascular endothelium resulting in improved tumor control. In several prostate cancer cells, as in many cancer cells, there is constitutive activation of Akt. Furthermore, there is significant amount of evidence that multiple receptor tyrosinse kinases may be aberrantly activated in the prostate cancer cells. Therefore, we sought to study the effects of broad spectrum small molecule tyrosine kinase inhibitors in the prostate tumor models. We hypothesized that inhibition of this RTK/PI3K/AKT pathway will result in radiosensitization of prostate tumors via dual effect on both the tumor cells, and its microvasculature. Furthermore, by innovative approach of molecular profiling using state of the art proteomic technology (Matrix Assisted Laser Desorption Ionization or MALDI-imaging), we hypothesize that we can identify tumors with a molecular profile that are predictive of response to TKI and radiation therapy (RT). The techniques established in this study to determine the pharmacokinetics and molecular profile to TKI, can be applicable to other therapeutic agents. Our goal is for the results of these preclinical studies to provide mechanistic insights for the formulation of clinical studies aimed at taking these promising pipeline compounds to help treat patients with high risk prostate cancer.

Abbreviations:
EGFR = Epidermal Growth Factor Receptor
IR = Ionizing Radiation
IP = Intraperitoneal
MALDI = Matrix Assisted Laser Desorption Ionization
uM = microMolar
nM = nano Molar
PSA = Prostate Specific Antigen
RT = Radiation Therapy
TKI = Tyrosine Kinase Inhibitor
VEGFR = Vascular Endothelial Growth Factor Receptor

Body

Synthesis – Year 2

In the second year, we have synthesized information/data formulated in year 1, having repeated and verified reproducibility of the previous experiments. Furthermore, we extended our work in to a second cell line model – PC3 prostate cancer cells. We have determined that differential expression of the two models (PC-3 vs. DU145 cells) of the EGFR expression appears to lead to sensitivity of these cells to combined therapy with EGFR/VEGFR blockade and radiation therapy. The synthesis of this work has been produced into a publication, which was recently submitted to the International Journal of Radiation Oncology Biology, Physics, and is currently in review. This publication is attached below as our summary of year 2's accomlishments in the following page.

Title: Differential efficacy of combined therapy with radiation and AEE788 in a high and low EGFR expressing androgen independent prostate tumor models.

ABSTRACT:

Purpose: To determine the efficacy of combining radiation (XRT) with a dual EGFR/VEGFR inhibitor, AEE788, in prostate cancer models with different levels of EGFR expression.

Methods and Materials: Immunoblotting was performed for EGFR, phosphorylated-EGFR (p-EGFR), and p-AKT in prostate cancer cells. Clonogenic assays were performed on DU145, PC-3 and HUVEC cells treated with XRT+/-AEE788. Tumor xenografts were established for DU145 and PC-3 on hindlimbs of athymic nude mice assigned to four treatment groups: 1) Control, 2) AEE788, 3) XRT, 4) AEE788+XRT. Tumor blood flow and growth measurements were performed using immunohistochemistry and imaging.

Results: AEE788 effectively reduced p-EGFR and p-AKT levels in DU145 and PC-3 cells. Clonogenic assays showed no radiosensitization for DU145 and PC-3 colonies treated with

AEE788+XRT. However, AEE788 caused decreased proliferation in DU145 cells. AEE788 showed radiosensitization effect in HUVEC and increased apoptotis susceptibility. Concurrent AEE788+XRT compared to either alone led to significant tumor growth delay in DU145 tumors. In contrast, PC-3 tumors derived no added benefit to combined modality therapy. In the DU145 tumors, significant reduction in tumor blood flow with combination therapy was demonstrated by power Doppler sonography and tumor blood vessel destruction on immunohistochemistry. MS imaging demonstrated that AEE788 is bioavailable and heterogeneously distributed in DU145 tumors undergoing therapy.

Conclusion: AEE788+XRT showed efficacy in *vitro/in vivo* with DU145-based cell models while PC-3-based were adequately treated with radiation alone without added benefit from combination therapy. These findings correlated with differences in EGFR expression and demonstrated effects on both tumor cell proliferation and vascular destruction.

INTRODUCTION

Prostate cancer is the second leading cause of cancer death in men with an estimated 230,090 men diagnosed with prostate cancer in 2005 (1). The first line of therapy includes surgery or radiation therapy (XRT) (2-4), with intermediate to high risk patients often receiving androgen suppression therapy (5). Once the disease progresses to an androgen independent disease status (AID), therapeutic options for prostate cancer patients diminish, with an overall survival of 6-12 months (6). Chemotherapy confers only a small survival benefit in patients with metastatic prostate cancer (7, 8), suggesting a need for investigation of non-hormonal systemic therapy. In AID patients, combining radiation with systemic agents result in 20-30% therapy failure (9), therefore requiring better treatment approaches.

Studies have demonstrated that human prostate cancer cells (DU145 and PC-3) derived from androgen independent prostate tumors express epidermal growth factor receptor (EGFR) (10-13). Furthermore, in pre-clinical studies involving various cancer models, including prostate tumors, EGFR overexpression has been linked to proliferation, angiogenesis, and migration (14-16), and

has an inverse relationship to tumor radiocurability (17, 18). In prostate cancer, EGFR expression correlates with higher Gleason score, higher PSA values, and is an independent prognostic factor negatively impacting disease free survival (19). New small molecule drugs targeting the EGFR receptor have been developed and show promise in the clinical setting. For head and neck cancer, combining ionizing radiation with EGF signal blockade conferred statistically significant survival benefit in a large randomized phase III study (20).

In addition to targeting EGFR, the use of vascular endothelial growth factor receptor (VEGFR) inhibitors is actively being investigated for cancer therapy (21). In fact, a number of preclinical studies have demonstrated that molecular compounds targeting VEGFR-2 (such as SU11248) when combined with radiation leads to improved tumor growth delay, partially due to significant tumor vascular destruction (22). Since there is a direct correlation between angiogenesis as well multiple angiogenesis related proteins with tumor grade (high Gleason Score), tumor stage, progression of disease, metastatic potential and survival (23, 24), analysis of angiogenesis-related proteins has been examined. In particular, VEGFR-2 expression has been reported suggesting that prostate tumors are highly vascular and may also benefit from therapy targeting VEGFR-2 (25). Furthermore, a recent study has suggested a significant advantage to combining both EGFR and VEGFR inhibitors *in vitro* to reduce the activation of Akt in endothelial cells (26).

The development of AEE788, a dual tyrosine kinase inhibitor of both EGFR and VEGFR, now provides an avenue to investigate the effect of simultaneous blockade of EGFR and VEGFR (27-35) when combined with conventional cytotoxic agents such as radiation. We hypothesized that dual inhibition of both targets (EGFR and VEGFR) using AEE788 in prostate cancer models should lead to improved tumor control when combined with radiation.

METHODS AND MATERIALS

Cell Culture, Animals, and Compounds

DU145 and PC-3 (ATCC, Rockville, MD) human prostate cancer cells and Human umbilical vein endothelial cells (HUVEC) were obtained from Cambrex (East Rutherford, NJ), and cultivated *in vitro* according to the recommendations of the supplier. Five to six week old male athymic nude mice (nu/nu) were purchased from Harlan Laboratories and maintained in accordance to guidelines approved by the Vanderbilt Institutional Animal Care and Use Committee (IACUC). AEE788 was provided by Novartis Pharma (Basel, Switzerland). For cellular assays, AEE788 was dissolved in DMSO, and for *in vivo* experiments, AEE788 was dissolved in a suspension on N-methylpyrroline and PEG300 1:9 (v/v).

Western Blots

DU145 and PC-3 cells were grown in 100 mm dishes to 90% confluency. Cells were serum starved overnight and treated with DMSO (control) and AEE788 (500 nM or 1 μM) for 2 hours and then stimulated with EGF (100 ng/ml) for 15 minutes at 37°C/5% CO2. Cells were washed twice in PBS and lysed with M-PER (Pierce) supplemented with phosphatase cocktail inhibitor mix and protease inhibitor cocktail mix (Sigma) according to the manufacturer recommendations at 4°C for 5 min prior to harvest. Remainder of the procedure has been described previously (22). Primary antibodies used were rabbit polyclonal antibodies for phophorylated-EGFR (Tyr 1068, 1:500), EGFR (1:1000), phosphorylated-AKT (Se473, 1:1000), and AKT (1:1000) from Cell Signaling Technology (Beverly, MA) and monoclonal anti-Actin (1:5000) from Santa Cruz Biotechnologies.

Clonogenic Assay

DU145, PC-3 and HUVEC cells were seeded in triplicate and distributed in different treatment groups: Control (DMSO) and AEE788 (100 nM, 500 nM, and 1 μM) +/- radiation (0, 2, 4, and 6 Gy). Drug treatment was applied 2 hours prior to radiation treatment. Colonies were allowed to grow for 2 weeks prior to harvesting and assay performed as previously described (22).

In vitro cell proliferation assay

DU145 and PC-3 cells were plated in duplicate at $1x10^4$. The experimental groups were treated with 100 nM, 500 nM and 1 μM AEE788 dissolved in DMSO as well as a control group (DMSO). Cells were counted using a Coulter counter at days 0, 2, 4, and 6.

Annexin V labeling by flow cytometry

HUVEC cells were plated at 50-60% confluency for each treatment. Cells were starved with MCDB medium (GIBCO) containing 0.2% BSA for six hours prior to adding 1μM AEE788, and incubated for 4 hours prior to and XRT (6 Gy) using a Therapax DXT 300 X-ray machine (Pantak). All cells were harvested 24h post irradiation. 5 μM Camptothecin was used as a positive control for apoptosis. The supernatant and adherent cells were both collected, and then prepared per manufacturer's instructions to perform Annexin V assay (BD Biosciences, San Jose CA). Annexin binding was read with 488 nm at a standard configuration and PI was read with 532 nm lasers having excitation power output lowered to 25 mW. Analysis was performed by calculating the fraction of cells in each of the four gating windows.

Xenograft Models and Therapy

$3.5x10^6$ cells (DU145) or $5x10^6$ cells (PC-3) were injected subcutaneously in the right hind-limbs of 30 athymic nu/nu mice. Three weeks post-injection, all mice were randomized in four treatment groups (n=5): (1) control, (2) AEE788 (25 mg/Kg), (3) XRT (2-3 Gy), and (4) AEE788+XRT. Animals received vehicle (N-methylpyrroline and PEG300 1:9 v/v) or 25 mg/kg of AEE788 by oral gavage for 7 days, two hours prior to radiation (3 Gy x 7 days). The (a) length, (b) width and (c) depth, of tumors were measured every 2 days, and tumor volumes were calculated from the formula (a x b x c)/2 derived from the ellipsoid formula.

Immunohistochemistry and TUNEL

Paraffin-embedded prostate cancer xenograft tissues collected from mice receiving 5 consecutive days of treatment (AEE788+/-XRT) were sectioned (5 μm) and used to detect expression of Ki-67, and co-localization of von Willebrand Factor (VWF) and TUNEL. Paraffin was removed from the slides and tissue sections were rehydrated. Endogenous peroxidase was neutralized with 0.03% hydrogen peroxide followed by a casein-based protein block (DakoCytomation, Carpinteria, CA) to reduce nonspecific staining. The sections were incubated for 30 min with rabbit anti-human VWF (1:900, Dakocytomation, Carpenteria, CA) after antigen retrieval with proteinase K and rabbit anti-human Ki-67 (1:1000, NovaCastra Laboratories Ltd., Newcastle, UK). Sections without primary antibody served as negative controls. The Dako Envision+ HRP/DAB System (DakoCytomation) was used to produce localized, visible staining. TUNEL staining was performed following vendor specifications (DeadEnd Colorimetric TUNEL System, Promega, Madison, WI). For co-staining procedure, TUNEL was performed after staining to localize VWF. The slides were lightly counterstained with Mayer's hematoxylin, dehydrated and coverslipped.

Ultrasound Imaging

Prostate tumors (DU145 and PC-3) underwent power Doppler sonography prior to therapy and after five consecutive days of daily therapy. Tumors were imaged with a 10-5 MHz linear probe (Entos, Philips/ATL, Bothell, WA) attached to a US scanner (HDI 5000, Philips/ATL). A tumor cross-section consisting of at least 20 power Doppler US images was acquired in real time with a gain of 82%. Care was taken to minimize motion artifact during the scan. Data from power Doppler ultrasound imaging was analyzed as described previously (36).

MALDI

Frozen prostate tumor xenograft tissue samples corresponding to each treatment group: (a) control, (b) 25 mg/kg AEE788 (c) 25 mg/kg AEE788 + XRT (3 Gy), were harvested at 24 h and after 5 days of consecutive treatment, prepared, and MALDI-TOF mass spectra were acquired on a Voyager DE-

STR mass spectrometer (Applied Biosystems, Foster City, CA, USA) following specifications previously described (37, 38).

Statistical Analysis

All descriptive statistics including means and standard error of means (SEM) were performed. Unpaired student t-test were used to evaluate differences between control group and each treatment group in all *in vitro* and *in vivo* studies performed.

RESULTS

Differential Expression of EGFR in two prostate cancer cell lines

EGFR expression in prostate cancer cell lines, DU145 and PC-3, was assessed using immunoblot analysis. At baseline, there was a higher level of EGFR protein expression in the DU145 cells compared to the PC-3 cells (Fig. 1). When serum starved, only a faint level of phosphorylated EGFR activity was noted in both cell lines (Fig. 1, lanes 1 and 5). Treatment with recombinant human EGF (100 ng/mL) led to robust phosphorylation of EGFR in the DU145 cells (Fig. 1, lane 6), and only minimal induction of phosphorylation of EGFR in the PC-3 cells (lane 2). Pretreatment with AEE788, 2 hours prior to EGF treatment, led to abrogation of the EGFR phosphorylation in both prostate cancer cell lines (lanes 3 and 7). This inhibition, as expected, was much more apparent in the DU145 cells.

The highly EGFR expressing DU145 cells have reduced colony size when treated with AEE788 compared to the PC-3 cells

Clonogenic survival assay was performed on both DU145 (Panel A) and PC-3 (Panel B) cells by treating them with increasing doses of ionizing radiation (0, 2, 4, 6 Gy) and AEE788 (0, 500 nM, 1 μM). Both prostate cancer cells demonstrated no impact on surviving fraction for up to 1 μM AEE788 doses (Fig. 2A.1, 2B.1). However, a reduction in individual surviving colony size was noted in

DU145 cells, with no uniform reduction in colony size in PC-3 cells with the same dose of AEE788 treatment (data not shown). This data suggests that inhibition of EGFR impacts the proliferation rate of DU145 cells more so than the PC-3 cells. Interestingly, the lower EGFR expressing PC-3 cells were more sensitive to radiation treatment alone than the DU145 cells (Fig. 2A.1, 2B.1). These results indicate that while there is no significant radiosensitizing effect of AEE788 on both cells, in the highly EGFR expressing DU145 cells, inhibition of EGFR phosphorylation may lead to decreased proliferation rate of the cells that survive radiation therapy.

AEE788 leads to increased inhibition of cell proliferation in the DU145 cells

EGFR expression has often been linked with cell proliferation (14-16). Therefore, we studied the impact of EGFR inhibition on DU145 and PC-3 cell proliferative capacity. Cells were seeded in normal culture conditions, on day 0, and treated with 0, 100, and 500 nM AEE788 compound. Cells were harvested at days 2, 4, and 6 following treatment. As seen in Fig. 2A.2, there was a dose dependent reduction in cell numbers for the DU145 cells. Interestingly, even at the lower dose of 100 nM concentration, there was a reduction in cell proliferation for the DU145 cells ($p=0.062$). The PC-3 cells only displayed a modest reduction (Fig. 2B.2, $p=0.174$) even at the higher 500 nM concentration of AEE788 treatment. These data suggest that inhibition of EGFR activity had a greater impact on cell proliferation for the highly EGFR expressing DU145 cells.

AEE788 therapy when combined with XRT leads to clonogenic radiosensitization and increased apoptosis in HUVEC

We next investigated the effect of AEE788+XRT in tumor vasculature endothelial cells. Combination therapy of AEE788 and radiation in human umbilical vein endothelial cells (HUVEC) resulted in significant reduction (*$p=0.001$) in the surviving fraction compared to radiation (XRT) alone (Fig. 3A). To further define the cytotoxic effect of AEE788 in HUVEC, we performed flow cytometry assessment of annexin V staining as a marker of apoptosis in HUVEC treated with

AEE788 or vehicle +/-XRT. Treatment with AEE788 (p=0.128) or XRT (p=0.152) alone did not confer significant apoptosis. However, treatment with AEE788 in combination with XRT led to more than additive levels of endothelial cell apoptosis (Fig. 3B, 3C, * p=0.002 compared to XRT). Endothelial cell apoptosis induction by combination therapy of AEE788 and XRT may be a primary mechanism for the radiosensitization effect noted on the clonogenic assay (Figure 3A).

Prostate xenograft tumor growth delay is increased in combination therapy group (AEE788+XRT) for DU145 prostate tumor models

Optimal doses for AEE788 therapy in preclinical studies have been established (50 mg/Kg), when used as a single agent(29). For our studies, we investigated a lower dose (25 mg/kg) of AEE788 as doses needed for radiosensitizing effects are often lower than what is required for single agent activity, and often less toxic. Treatment groups included: 1) AEE788 (25 mg/kg), 2) XRT (2-3Gy), 3) XRT (2-3Gy) +AEE788 (25 mg/kg) 4) no treatment delivered consecutively for seven days. Tumor volumes were measured for up to 40 days after initiation of therapy. In the DU145 xenograft tumors, there was a marked increase in tumor growth delay in the animals that were treated with AEE788+XRT (Fig. 4A) compared to radiation alone (*p=0.044 compared to XRT). AEE788, even at the lower dose (25 mg/kg), was effective at inducing modest tumor growth delay in this model. In contrast, in the PC-3 xenografts (Fig. 4B), the lower dose of AEE788 did not confer a significant tumor growth delay. When these tumors were treated with 3 Gy x 7 doses, there was near complete abrogation of tumor growth (data not shown), correlating well with the higher radiosensitivity of these tumors seen in the clonogenic assays *in vitro*. Therefore, in order to determine whether there is any added benefit of the drug with radiation treatment, we reduced the radiation dose to 2 Gy per day x 7 fractions. Despite this reduction, in PC-3s, XRT alone and the AEE788+XRT treated group showed very similar tumor growth rate (Fig. 4B, ** p=0.727), suggesting no additional benefit conferred by the drug to the cytotoxic effects of radiation.

Combination therapy of AEE788 and XRT leads to significant reduction in tumor blood flow in the DU145 tumors

The same animals which were subjected to tumor volume measurement analysis in Fig. 4A were also measured longitudinally for tumor blood flow using non-invasive Doppler Ultrasound as we have done previously (36, 39). As demonstrated in Fig. 5A, animals that were treated with XRT and AEE788 demonstrated statistically significant decrease in tumor blood flow compared to day 0 as assessed by percent change in power weighted pixel density (PWPD) measurements (p=0.03). Animals treated with either vehicle, AEE788, or XRT alone did not demonstrate significant reduction in tumor blood flow (p=0.2, p=0.7, and p=0.5, respectively). Meanwhile, in the PC-3 tumor xenografts undergoing same treatment conditions, there was no significant reduction, but rather a slightly increased level in tumor blood flow at 5 days following AEE+XRT treatment (p=0.1) (figure 5 A.1 lower panel, p= 0.1). In fact, in all of the PC-3 groups (vehicle control treatment, AEE788 or XRT monotherapy), after 5 days of treatment, the tumor blood flow levels were increased compared to baseline levels, suggesting that AEE788 with or without radiotherapy failed to reduce tumor blood flow levels (figure 5.A.1 lower panel).

DU145 prostate tumor xenograft treated with combination therapy (AEE788+XRT) have reduced microvessel density, increased endothelial cell apoptosis, and reduced proliferative capacity

To confirm the Doppler ultrasound findings, we examined the vasculature of treated tumors immunohistochemically. Microvessel density (MVD) was assessed in DU145 tumors after 5 days of consecutive treatment with AEE788+/-XRT, measured by counting number of von Willibrand Factor (VWF) positive cells present in 10 random high power fields. Co-staining of VWF and TUNEL was also performed in same tissue sections to assess for apoptotic endothelial cells *in vivo*. Microvessel density of tumors within animals treated with AEE788 + XRT was significantly reduced compared to control animals (8.86 +/- 0.11 and 14.15+/-0.93 respectively, p=0.004). In comparison, monotherapy with AEE788 or XRT on tumors did not display a significant reduction in MVD

compared to untreated control animals (14.55+/-2.49 and 12.32+/-2.36, p=0.88 and 0.51, respectively) (Fig. 5B and Table 1). When level of apoptotic blood vessels was assessed in the treated tumors, all three treatment regimens, AEE788 (48.67+/-4.05), XRT(49.67+/-2.19), and AEE788 +XRT (61.67+/-3.84) led to a statistically significantly elevation in blood vessel apoptosis compared to control (22.00+/-2.08)(p=.004, p=.0007, and p=.0008, respectively) (Fig. 5B and Table 1). Moreover, there was a statistically significant elevation of apoptotic blood vessels in the AEE788+XRT group when compared to the XRT group (p=.05). When compared to the AEE788 treatment group, the tumors in the AEE788+XRT group displayed a trend for increased blood vessel apoptosis (p=0.08).

To assess for proliferative capacity of the tumors following 5 days of consecutive treatment with AEE788+/-XRT, Ki-67staining was performed in DU145 prostate tumors. The tumors treated with both AEE788 and XRT (165.77+/-25.12) had a statistically significant reduction in Ki-67 staining compared to the untreated tumors (285.36+/-16.25) (p=.016) (Fig. 5C, and Table 1). However, tumors treated with AEE788 (158.57+/-31.78) or XRT (195.62+/-20.9) alone also showed significant reduction in Ki-67 staining compared to control tumors (p=0.024 and p=0.028, respectively) (Fig. 5C and Table1).

AEE788 is detected using MALDI-imaging in prostate tumors

To determine whether AEE788 bioavailability in prostate tumors correlates with tumor blood flow reduction data (Fig 5A, 5A.1), we used MALDI-imaging, a technology that has been used to determine a drug's spatial biodistribution directly from frozen tissue sections(37). The bioavailability of AEE788 in DU145 prostate tumor xenograft sections was determined at various time points following oral administration of the compound. *In vitro,* AEE788 is ionized and detected in fragments at two specific sites with mass to charge (M/Z) ratios of 223 and 327 (Fig.6A). DU145 prostate xenograft tumors sections were imaged for AEE788 (m/z 327, represented as blue pixels) at 24 h (Fig 6B lane 2), and after 5 days of consecutive therapy (Fig. 6B lanes 3-4). As seen in Fig.

6B lane 2, there was a sustained heterogeneous distribution of the AEE788 compound even 24 h post administration. This provides favorable pharmacokinetics for its use in combination with radiation therapy. Combined therapy with AEE788+XRT which led to tumor blood vessel destruction (Figure 5A), also demonstrated a reduction in the biodistribution of AEE788 in prostate tumors (Fig. 6B.lane 4). Tumor that was treated with vehicle demonstrates no AEE788 signal as expected (Fig. 6B lane 1).

DISCUSSION

Receptor tyrosine kinase targeting, especially EGFR, is an anti-cancer strategy being actively investigated. FDA approved drugs for clinical use in cancer therapy targeting VEGF , VEGFR, and EGFR are clinically available (11, 40). Several clinical studies of combination of these drugs with ionizing radiation, has demonstrated safety and potential efficacy of this regimen (20). AEE788 has a potential advantage as it inhibits both EGFR and VEGFR (29). Since EGFR and VEGFR expression has shown to be important for prostate cancer biology (12, 19, 25, 41), there is significant rationale for treatment of these tumors with AEE788.

This study demonstrated differential response to combining radiation therapy with dual inhibitor of EGFR and VEGFR, in human prostate cancer models. Previous studies have shown presence of higher EGFR expression in prostate cancers derived from androgen-independent prostate tumors (10-13). The two human prostate cancer cell lines chosen in our study, DU145 and PC-3, are both androgen-independent tumors. However, there is a differential expression of EGFR and phosphorylation level in these two cell lines being high for DU145 and low for PC-3 (Fig. 1). Interestingly, the two tumors demonstrated differential growth rates with a higher proliferation rate for DU145 cells and lower proliferation for PC-3 cell (Fig 2A, 2B, 4). In the highly EGFR expressing DU145 cells, blockade of EGFR with AEE788 led to growth inhibition, which was not observed in the PC-3 cells. This suggests that EGFR levels in these androgen independent tumor cells are directly related to their proliferative capacity.

Treatment with AEE788, however did abrogate the phosphorylation of EGFR in both cell lines. There was a strong downregulation of the EGFR downstream target p-AKT in both DU145 and PC-3 cell lines. Interestingly, there was a robust activation of AKT even in PC-3 cells following serum starvation and EGF stimulation (100 ng) which is consistent with a previously published report (12). Although some have reported little to no difference in p-AKT for basal and serum starved PC-3 cells subject to EGF stimulation (42), the dose of EGF used in such studies was lower (50 ng) than the present study. Although the constitutive phosphorylation of downstream proteins, such as AKT in PC-3 is likely due to the PTEN negative status(42), our data indicates that EGF stimulation does enhance this AKT phosphorylation. The noted improved treatment efficacy with AEE788 in the DU145 cells that have high EGFR expression suggests that efficacy of EGFR targeted compounds may be dependent on cell's EGFR level and activity.

Previously, pre-clinical studies using ZD1839, an EGFR inhibitor, with standard chemotherapeutics demonstrated growth inhibition when used at high doses in LNCaP, DU145 and PC-3 prostate xenografts (42, 43). The lower doses of AEE788 chosen in our study were effective due to radiosensitization effect, primarily on the vasculature, but also likely due to anti-proliferative effect on the highly expressed EGFR levels in the DU145 tumor. Therefore, it appears that lower drug doses can be used when used as a radiosensitizer in appropriately selected tumors.

Based on our studies, the anti-vascular effect of radiation and AEE788 predominated. The endothelial cells displayed significant radiosensitization to increasing doses of AEE788 by our *in vitro* assays (Fig 3). Furthermore, in DU145 tumor xenografts, we found both histological and imaging (Doppler ultrasound) evidence of effective vasculature destruction following combined AEE788 and radiation treatments. A recent study has suggested the notion that HUVEC express phosphorylated-EGFR when subject to radiation and expression is abrogated by use of both EGFR and VEGFR inhibitors (26). In contrast, the PC-3 tumors vasculature did not respond to AEE788 with or without XRT. It is unclear why AEE788 failed to sensitize the PC-3 vasculature to the

cytotoxic effects of radiation, but it leads one to speculate that the tumor type has a direct impact on host (vasculature)'s response to targeted therapy.

Finally, the data suggests that not all prostate tumors will be effectively radio-sensitized by EGFR and VEGFR blockade. The findings correlate to a previous report using the EGFR inhibitor, ZD1839, in PC-3 prostate xenografts whereby ZD1839 failed to downregulate PI3K/AKT activity (43); PC-3 cells maintained their phosphorylated-AKT expression due to their PTEN negative status. Identification of biomarkers which can predict for targeted therapy sensitivity may become clinically relevant. MALDI-TOF technology utilized in our studies holds promise to help in identification of such biomarkers.

CONCLUSION

The data presented supports the efficacy of AEE788 in DU145 prostate tumors. These studies further indicate that even lower doses of AEE788 combined with ionizing radiation can lead to significant tumor growth delay in the highly EGFR expressing DU145 prostate tumors. In contrast, the slower growing PC-3 tumors were sensitive to radiation therapy alone and AEE788 did not confer any added benefit. Two independent mechanisms may play a role in improving prostate cancer therapy when AEE788 is combined with radiation in the highly EGFR expressing tumors: (1) by promoting tumor vasculature destruction and (2) by decreasing proliferation of tumor cells surviving cytotoxic effects of radiation therapy.

References

1. Jemal A, Ward E, Wu X*, et al.* Geographic patterns of prostate cancer mortality and variations in access to medical care in the United States. *Cancer Epidemiol Biomarkers Prev* 2005;14:590-595.
2. Loberg RD, Logothetis CJ, Keller ET*, et al.* Pathogenesis and treatment of prostate cancer bone metastases: targeting the lethal phenotype. *J Clin Oncol* 2005;23:8232-8241.
3. Macvicar GR, Hussain M. Chemotherapy for prostate cancer: implementing early systemic therapy to improve outcomes. *Cancer Chemother Pharmacol* 2005;56 Suppl 1:69-77.
4. Speight JL, Roach M, 3rd. Radiotherapy in the management of clinically localized prostate cancer: evolving standards, consensus, controversies and new directions. *J Clin Oncol* 2005;23:8176-8185.
5. Auclerc G, Antoine EC, Cajfinger F*, et al.* Management of advanced prostate cancer. *Oncologist* 2000;5:36-44.
6. Tannock IF, Osoba D, Stockler MR*, et al.* Chemotherapy with mitoxantrone plus prednisone or prednisone alone for symptomatic hormone-resistant prostate cancer: a Canadian randomized trial with palliative end points. *J Clin Oncol* 1996;14:1756-1764.
7. Petrylak DP, Tangen CM, Hussain MH*, et al.* Docetaxel and estramustine compared with mitoxantrone and prednisone for advanced refractory prostate cancer. *N Engl J Med* 2004;351:1513-1520.
8. Tannock IF, de Wit R, Berry WR*, et al.* Docetaxel plus prednisone or mitoxantrone plus prednisone for advanced prostate cancer. *N Engl J Med* 2004;351:1502-1512.
9. Cheung R, Kamat AM, de Crevoisier R*, et al.* Outcome of salvage radiotherapy for biochemical failure after radical prostatectomy with or without hormonal therapy. *Int J Radiat Oncol Biol Phys* 2005;63:134-140.

10. Kumar VL, Majumder PK, Gujral S*, et al.* Comparative analysis of epidermal growth factor receptor mRNA levels in normal, benign hyperplastic and carcinomatous prostate. *Cancer Lett* 1998;134:177-180.

11. Chinnaiyan P, Varambally S, Tomlins SA*, et al.* Enhancing the antitumor activity of ErbB blockade with histone deacetylase (HDAC) inhibition. *Int J Cancer* 2006;118:1041-1050.

12. El Sheikh SS, Domin J, Abel P*, et al.* Phosphorylation of both EGFR and ErbB2 is a reliable predictor of prostate cancer cell proliferation in response to EGF. *Neoplasia* 2004;6:846-853.

13. Pu YS, Hsieh MW, Wang CW*, et al.* Epidermal growth factor receptor inhibitor (PD168393) potentiates cytotoxic effects of paclitaxel against androgen-independent prostate cancer cells. *Biochem Pharmacol* 2006;71:751-760.

14. Cross M, Dexter TM. Growth factors in development, transformation, and tumorigenesis. *Cell* 1991;64:271-280.

15. Olayioye MA, Neve RM, Lane HA*, et al.* The ErbB signaling network: receptor heterodimerization in development and cancer. *Embo J* 2000;19:3159-3167.

16. Prenzel N, Fischer OM, Streit S*, et al.* The epidermal growth factor receptor family as a central element for cellular signal transduction and diversification. *Endocr Relat Cancer* 2001;8:11-31.

17. Milas L, Fan Z, Andratschke NH*, et al.* Epidermal growth factor receptor and tumor response to radiation: in vivo preclinical studies. *Int J Radiat Oncol Biol Phys* 2004;58:966-971.

18. Nasu S, Ang KK, Fan Z*, et al.* C225 antiepidermal growth factor receptor antibody enhances tumor radiocurability. *Int J Radiat Oncol Biol Phys* 2001;51:474-477.

19. Di Lorenzo G, Tortora G, D'Armiento FP*, et al.* Expression of epidermal growth factor receptor correlates with disease relapse and progression to androgen-independence in human prostate cancer. *Clin Cancer Res* 2002;8:3438-3444.

20. Bonner JA, Harari PM, Giralt J*, et al.* Radiotherapy plus cetuximab for squamous-cell carcinoma of the head and neck. *N Engl J Med* 2006;354:567-578.

21. Ferrara N. Vascular endothelial growth factor: basic science and clinical progress. *Endocr Rev* 2004;25:581-611.

22. Schueneman AJ, Himmelfarb E, Geng L*, et al.* SU11248 maintenance therapy prevents tumor regrowth after fractionated irradiation of murine tumor models. *Cancer Res* 2003;63:4009-4016.

23. Charlesworth PJ, Harris AL. Mechanisms of disease: angiogenesis in urologic malignancies. *Nat Clin Pract Urol* 2006;3:157-169.

24. Padhani AR, Harvey CJ, Cosgrove DO. Angiogenesis imaging in the management of prostate cancer. *Nat Clin Pract Urol* 2005;2:596-607.

25. Jackson MW, Bentel JM, Tilley WD. Vascular endothelial growth factor (VEGF) expression in prostate cancer and benign prostatic hyperplasia. *J Urol* 1997;157:2323-2328.

26. Bozec A, Formento P, Ciccolini J*, et al.* Response of endothelial cells to a dual tyrosine kinase receptor inhibition combined with irradiation. *Mol Cancer Ther* 2005;4:1962-1971.

27. Kim S, Schiff BA, Yigitbasi OG*, et al.* Targeted molecular therapy of anaplastic thyroid carcinoma with AEE788. *Mol Cancer Ther* 2005;4:632-640.

28. Goudar RK, Shi Q, Hjelmeland MD*, et al.* Combination therapy of inhibitors of epidermal growth factor receptor/vascular endothelial growth factor receptor 2 (AEE788) and the mammalian target of rapamycin (RAD001) offers improved glioblastoma tumor growth inhibition. *Mol Cancer Ther* 2005;4:101-112.

29. Traxler P, Allegrini PR, Brandt R*, et al.* AEE788: a dual family epidermal growth factor receptor/ErbB2 and vascular endothelial growth factor receptor tyrosine kinase inhibitor with antitumor and antiangiogenic activity. *Cancer Res* 2004;64:4931-4941.

30. Younes MN, Yigitbasi OG, Park YW*, et al.* Antivascular therapy of human follicular thyroid cancer experimental bone metastasis by blockade of epidermal growth factor receptor and vascular growth factor receptor phosphorylation. *Cancer Res* 2005;65:4716-4727.

31. Yigitbasi OG, Younes MN, Doan D*, et al.* Tumor cell and endothelial cell therapy of oral cancer by dual tyrosine kinase receptor blockade. *Cancer Res* 2004;64:7977-7984.

32. Thaker PH, Yazici S, Nilsson MB*, et al.* Antivascular therapy for orthotopic human ovarian carcinoma through blockade of the vascular endothelial growth factor and epidermal growth factor receptors. *Clin Cancer Res* 2005;11:4923-4933.

33. Park YW, Younes MN, Jasser SA*, et al.* AEE788, a dual tyrosine kinase receptor inhibitor, induces endothelial cell apoptosis in human cutaneous squamous cell carcinoma xenografts in nude mice. *Clin Cancer Res* 2005;11:1963-1973.

34. Yokoi K, Kim SJ, Thaker P*, et al.* Induction of apoptosis in tumor-associated endothelial cells and therapy of orthotopic human pancreatic carcinoma in nude mice. *Neoplasia* 2005;7:696-704.

35. Yokoi K, Sasaki T, Bucana CD*, et al.* Simultaneous inhibition of EGFR, VEGFR, and platelet-derived growth factor receptor signaling combined with gemcitabine produces therapy of human pancreatic carcinoma and prolongs survival in an orthotopic nude mouse model. *Cancer Res* 2005;65:10371-10380.

36. Niermann KJ, Fleischer AC, Donnelly EF*, et al.* Sonographic depiction of changes of tumor vascularity in response to various therapies. *Ultrasound Q* 2005;21:61-67; quiz 149, 153-144.

37. Reyzer ML, Hsieh Y, Ng K*, et al.* Direct analysis of drug candidates in tissue by matrix-assisted laser desorption/ionization mass spectrometry. *J Mass Spectrom* 2003;38:1081-1092.

38. Reyzer ML, Caldwell RL, Dugger TC*, et al.* Early changes in protein expression detected by mass spectrometry predict tumor response to molecular therapeutics. *Cancer Res* 2004;64:9093-9100.

39. Schueneman AJ, Himmelfarb E, Geng L*, et al.* SU11248 maintenance therapy prevents tumor regrowth after fractionated irradiation of murine tumor models. *Cancer Res* 2003;63:4009-4016.

40. Halatsch ME, Schmidt U, Behnke-Mursch J*, et al.* Epidermal growth factor receptor inhibition for the treatment of glioblastoma multiforme and other malignant brain tumours. *Cancer Treat Rev* 2006;32:74-89.

41. Barton J, Blackledge G, Wakeling A. Growth factors and their receptors: new targets for prostate cancer therapy. *Urology* 2001;58:114-122.

42. Sirotnak FM, She Y, Lee F*, et al.* Studies with CWR22 xenografts in nude mice suggest that ZD1839 may have a role in the treatment of both androgen-dependent and androgen-independent human prostate cancer. *Clin Cancer Res* 2002;8:3870-3876.

43. Festuccia C, Muzi P, Millimaggi D*, et al.* Molecular aspects of gefitinib antiproliferative and pro-apoptotic effects in PTEN-positive and PTEN-negative prostate cancer cell lines. *Endocr Relat Cancer* 2005;12:983-998.

Figure Legends

Fig. 1. AEE788 attenuates prostate cancer response to EGF. Prostate cancer cells (DU145 and PC-3) were treated and subjected to Western blot analysis using antibodies for phospho-EGFR (p-EGFR), EGFR, phospho-AKT (p-AKT), AKT, and actin (loading control) for the indicated conditions. 1) PC-3 control cells (untreated), 2) PC-3 cells treated with 100 ng/mL EGF, 3) PC-3 cells treated with 500 nM AEE788 and 100 ng/ml of EGF, 4) PC-3 cells treated with 1000 nM AEE788 and 100 ng/ml of EGF, 5) DU145 controls (untreated), 6) DU145 cells treated with 100 ng/ml EGF, 7) DU145 cells treated with 500 nM AEE788 and 100 ng/ml EGF 8) DU145 cells treated with 1000 nM AEE788 and 100 ng/ml EGF.

Fig.2. AEE788 does not affect surviving fraction, however it impacts proliferation. *A.1*. Clonogenic assay of DU145 prostate cancer cells treated with AEE788 (500 nM, 1 μM)+/-XRT (2 Gy, 4 Gy, 6 Gy) as indicated. *A.2*. Cell proliferation assay of DU145 cells treated with increasing doses of AEE788 (500 nM and 1 μM). *B.1.* Clonogenic assay of PC-3 prostate cancer cells treated with AEE788 (500nM)+/-XRT (2, 4, 6 Gy) as indicated. *B.2.* Cell proliferation assay of PC-3 cells treated with increasing doses of AEE788 (500 nM and 1μM). * indicates p-values. SEM (Standard Error of Means).

Fig. 3. AEE788 enhances cytotoxicity in endothelial cells. *A.* Clonogenic assay of HUVEC treated with AEE788+/-XRT as indicated. *B, C*. Apoptosis assay via flow cytometry for Annexin V and propidium iodide with or without XRT (0 or 6 Gy), treated with AEE788 (0 or 1 μM) as indicated, * indicates p-values. SEM (Standard Error of Means).

Fig. 4. AEE788 treatment results in prostate tumor growth delay. DU145 (*A*) and PC-3 (*B*) xenografts tumors were treated as indicated were started when tumor reached ~ 800 mm^3 (21 days

after implantation for DU145 and 31 days for PC-3). AEE788 (25 mg/kg) was administered orally once per day for 7 days during the week of therapy. In AEE788+XRT and the XRT groups, 3 Gy for DU145 and 2 Gy for PC-3 was delivered to the mice hindlimbs containing the corresponding prostate tumor 2 hours after treatment with AEE788. Tumor volume was determined three times per week. N=5 for each treatment group. * indicates p-values. Red arrows indicate the end of the treatment protocol (day 7). SEM (Standard Error of Means).

Fig 5. AEE788+XRT results in tumor blood flow reduction, tumor microvessel destruction, and decreased proliferation. *A & A.1.* Tumor blood flow assessment was performed using Doppler ultrasonography at day 5 following indicated treatments. Doses for AEE788 and XRT were as described for figure 4 and in Materials and Methods. Graph depicts percent changes in PWPD at day 5 compared to day 0. *B.* Microvascular density and vasculature destruction (blue arrows) in DU145 tumors following 5 days of indicated treatments were assessed using immunohistochemical analysis. Double staining for microvasculature (anti-VWF antibodies) and apoptotic cells (TUNEL) was performed. *C.* Immunohistochemical analysis using anti-Ki67 antibodies on DU145 tumors 5 days following indicated treatments. SEM (Standard Error of Means).

Fig. 6. Imaging mass spectroscopy analysis of AEE788 biodistribution. *A.* Mass spectrometry analysis for AEE788. Ionized peaks detected at 327 and 223 m/z ratio represent AEE788. *B.* Spatial biodistribution of AEE788 in prostate cancer xenograft sections via MALDI-Q-TOF-MS. Bottom panels are MALDI-MS images of frozen DU145 prostate tumor tissue sections harvested at multiple time points after oral administration of AEE788 compound as indicated: lane 1) vehicle control treatment , lane 2) 24 hours post-treatment with 25 mg/kg AEE788, lane 3) AEE788 (25 mg/kg) for 5 consecutive days, lane 4) AEE788 (25 mg/kg)+XRT (3 Gy) for 5 consecutive days.

Fig. 1.

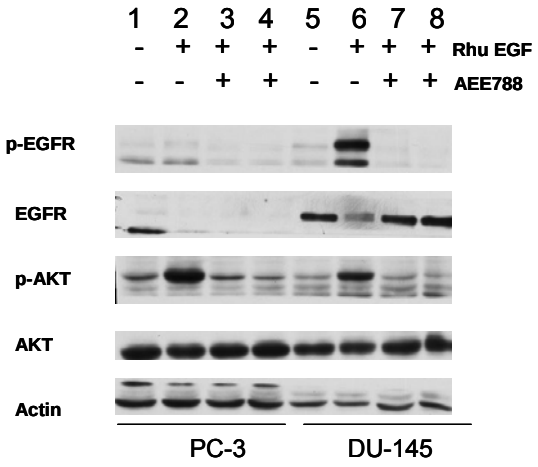
1 2 3 4 5 6 7 8
- + + + - + + + Rhu EGF
- - + + - - + + AEE788
p-EGFR
EGFR
p-AKT
AKT
Actin
PC-3
DU-145

Fig. 2.

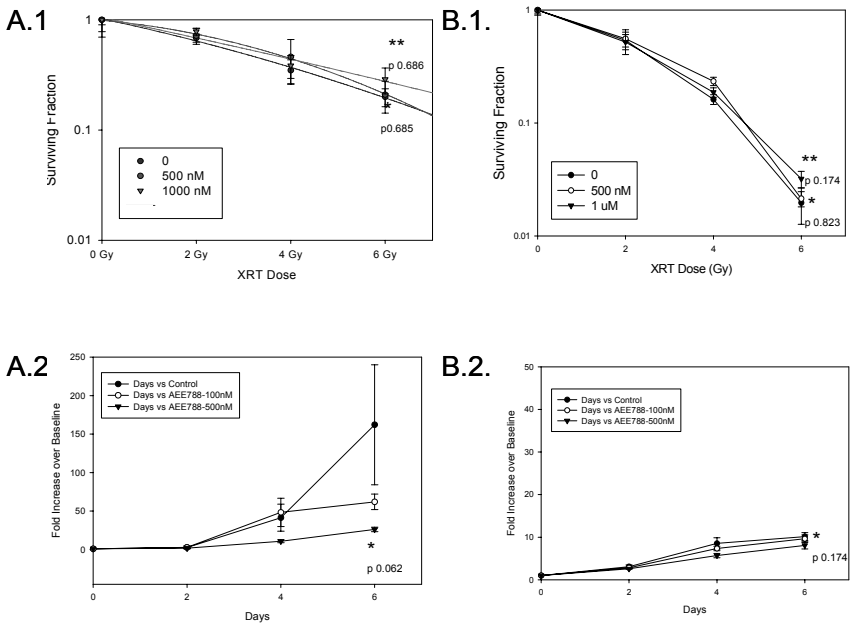
A.1
Surviving Fraction
XRT Dose
0 Gy
2 Gy
4 Gy
6 Gy
0
500 nM
1000 nM
p 0.686
p0.685
B.1.
Surviving Fraction
XRT Dose (Gy)
0
500 nM
1 uM
p 0.174
p 0.823
A.2
Fold Increase over Baseline
Days
Days vs Control
Days vs AEE788-100nM
Days vs AEE788-500nM
p 0.062
B.2.
Fold Increase over Baseline
Days
Days vs Control
Days vs AEE788-100nM
Days vs AEE788-500nM
p 0.174

Fig. 3.

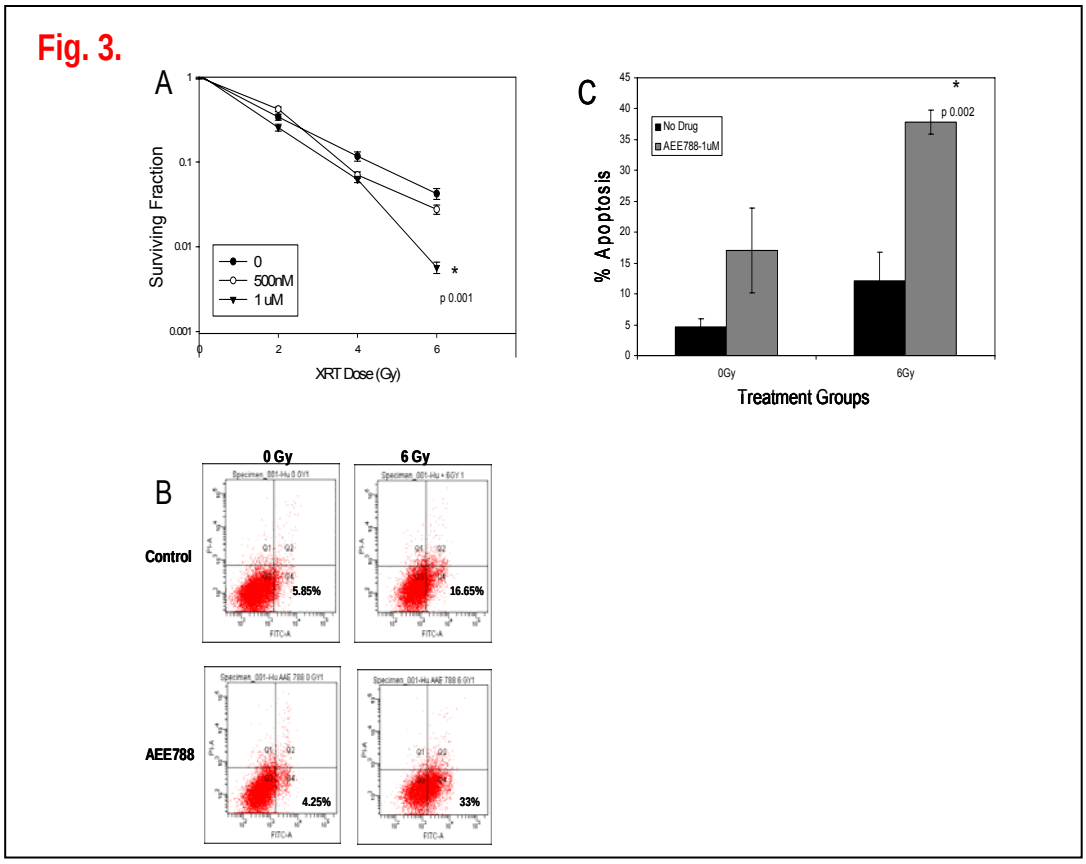
A
Surviving Fraction
1
0.1
0.01
0.001
0
2
4
6
XRT Dose (Gy)
0
500nM
1 uM
*
p 0.001
C
% Apoptosis
45
40
35
30
25
20
15
10
5
0
No Drug
AEE788-1uM
*
p 0.002
0Gy
6Gy
Treatment Groups
B
0 Gy
6 Gy
Control
5.85%
16.65%
AEE788
4.25%
33%

Fig. 4.

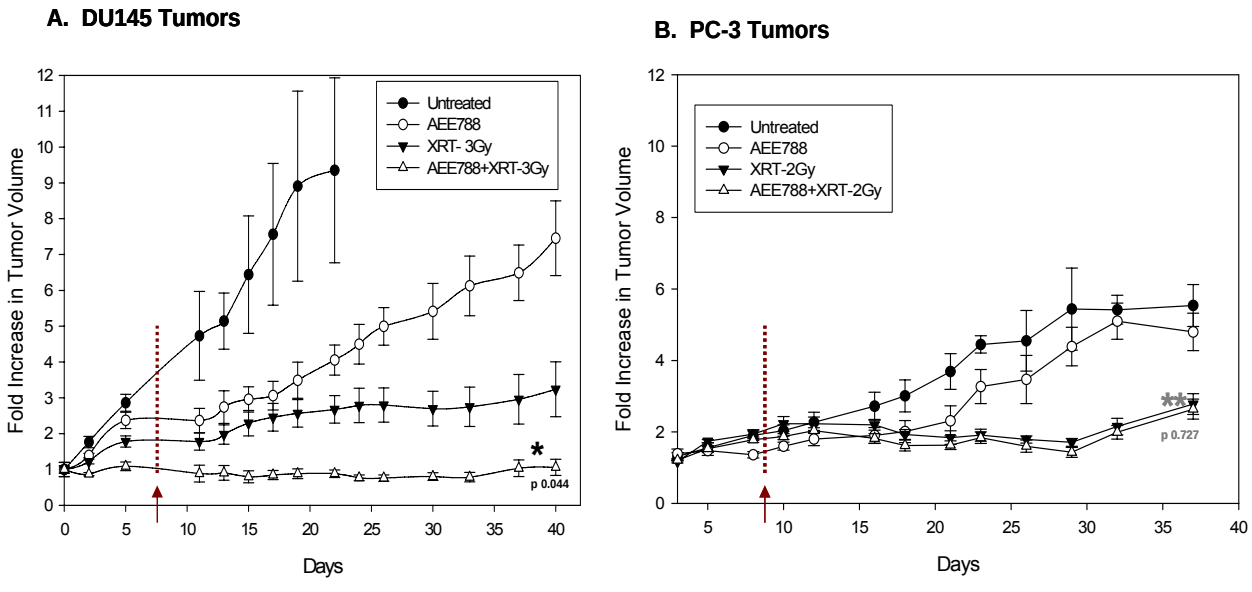
A. DU145 Tumors
Fold Increase in Tumor Volume
12
11
10
9
8
7
6
5
4
3
2
1
0
0
5
10
15
20
25
30
35
40
Days
Untreated
AEE788
XRT- 3Gy
AEE788+XRT-3Gy
*
p 0.044
B. PC-3 Tumors
Fold Increase in Tumor Volume
12
10
8
6
4
2
0
5
10
15
20
25
30
35
40
Days
Untreated
AEE788
XRT-2Gy
AEE788+XRT-2Gy
**
p 0.727

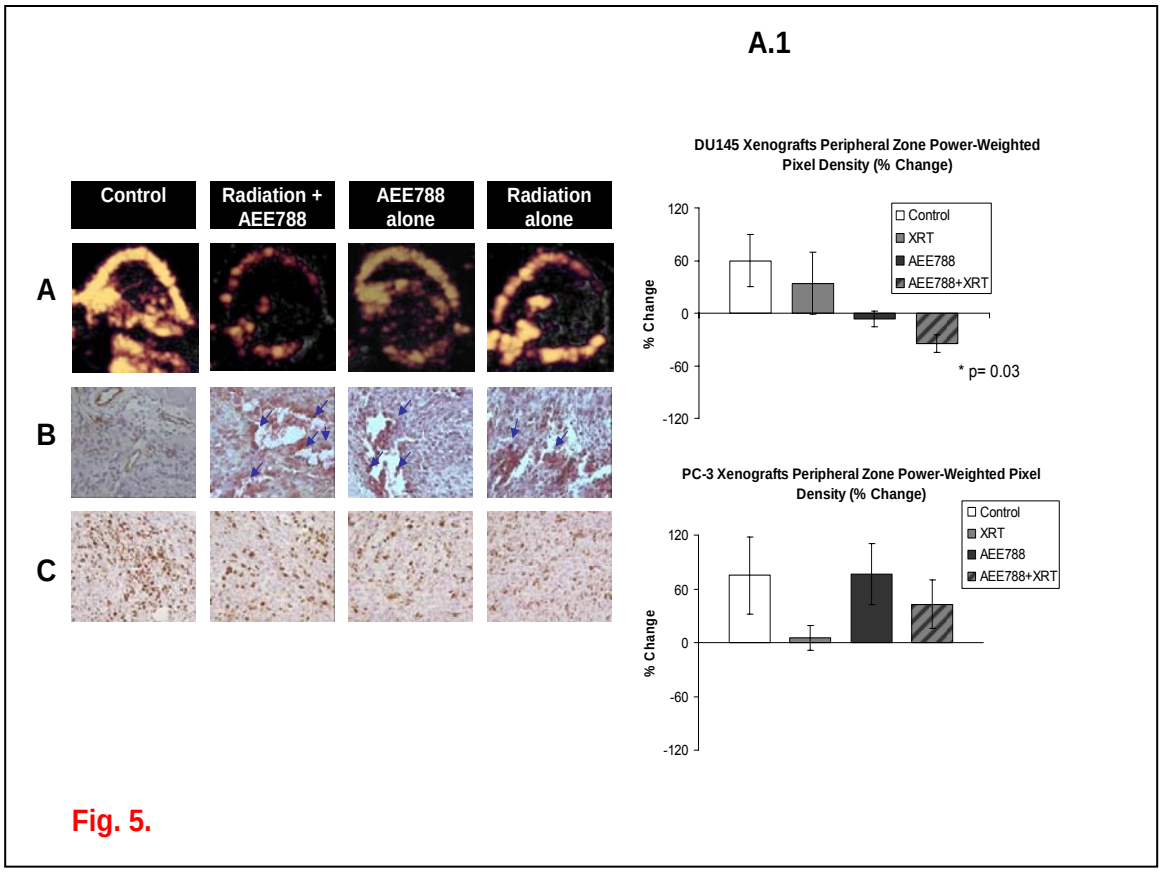
A.1
Control
Radiation + AEE788
AEE788 alone
Radiation alone
A
B
C
DU145 Xenografts Peripheral Zone Power-Weighted Pixel Density (% Change)
% Change
120
60
0
-60
-120
Control
XRT
AEE788
AEE788+XRT
* p= 0.03
PC-3 Xenografts Peripheral Zone Power-Weighted Pixel Density (% Change)
% Change
120
60
0
-60
-120
Control
XRT
AEE788
AEE788+XRT

Fig. 5.

Fig 6.

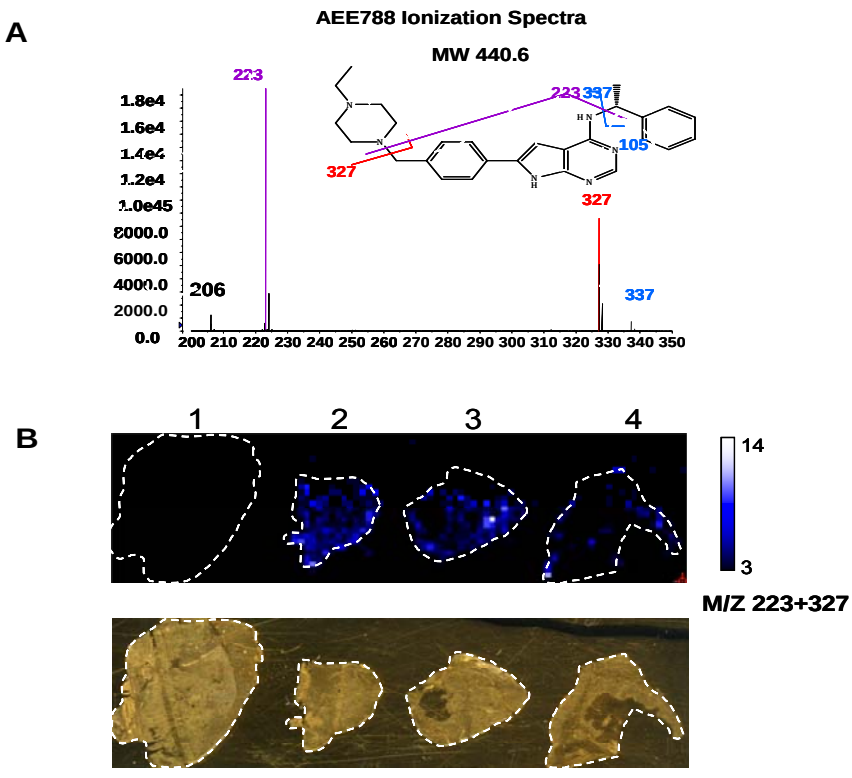
A
AEE788 Ionization Spectra
MW 440.6
223
223 337
105
327
327
337
206
1.8e4
1.6e4
1.4e4
1.2e4
1.0e45
8000.0
6000.0
4000.0
2000.0
0.0
200 210 220 230 240 250 260 270 280 290 300 310 320 330 340 350
B
1
2
3
4
14
3
M/Z 223+327

Key Research Accomplishments

- Abstract accepted for ASTRO (American Society of Therapeutic Radiation Oncology) Annual Meeting (2005) for poster discussion session where PI (Dong Kim) is the last author (first author is the research assistant working under Dong Kim on this DOD funded project).
    - **D.W. Kim**, J. Huamani, M. Reyzer, D. Mi, R. M. Caprioli, D. E. Hallahan. Imaging Mass Spectrometry to Map Distribution of Radiation Enhancing Vasculature Targeted Drug and Protein Biomarkers of Response to Therapy in Prostate Cancer. Poster Presentation, ASTRO 2006.
    - J. Huamani, K. Niermann, C.Willey, M. E. Reyzer, D. Thotala, L. Leavitt, C. Jones, A. Fleishcher, R. M. Caprioli, D. E. Hallahan, **D.W. Kim.** EGFR Activity Determines the Efficacy of Combined Therapy with Radiation and AEE788 in Prostate Cancer. Poster Presentation, ASTRO 2006.
    - J.Huamani, K.J. Niermann, M.L. Reyzer, J. Alberts, C. Jones, R. Caprioli, D.E. Hallahan, **D.W. Kim**. Combination Therapy of Ionizing Radiation with AEE788, a Dual Receptor Tyrosine Kinase Inhibitor Targeting Epidermal Growth Factor Receptor (EGFR) and Vascular Endothelial Growth Factor Receptor (VEGFR) Leads To Improved Tumor Control. Poster Discussion, ASTRO 2005.

- Abstract accepted for oral presentation for Radiological Society of North America (RSNA 2005) Annual meeting; P.I. also received RSNA Trainee Research Prize.
    - **D.W. Kim,** M.L. Reyzer, J. Huamani, K. J. Niermann, R. Caprioli, D.E. Hallahan. Direct Analysis of Protein Markers of Therapeutic Response in Tumors Treated with Radiation and Receptor Tyrosine Kinase Inhibitors (TKI) by Imaging Mass Spectrometry. RSNA 2005.

- Manuscript submitted for review:
    - **Differential efficacy of combined therapy with radiation and AEE788 in a high and low EGFR expressing androgen independent prostate tumor models.** First author: Jessica Huamani (Research Assistant supported through this grant); co-Corresponding Senior authorship – PI Dong Wook Kim, and Mentor Dennis Hallahan

- Technique for performing MALDI-imaging for receptor tyrosine kinase compounds including AEE788, SU11248 and Gleevec has been developed in collaboration with Vanderbilt Mass Spectrometry Resarch Center. Drug distribution analysis, as well as protein profiling of the tumors are now being performed using these established techniques.

Reportable Outcomes

1. Work supported by this grant is being presented in two poster presentations at ASTRO 2006, and as a poster discussion session at ASTRO 2005 national meeting (largest meeting for Radiation Oncologist).

2. Part of the work supported by this grant was presented as an ORAL PRESENTATION at RSNA 2005 national meeting (largest meeting for Radiologist). Dong Kim (P.I.) also received a Trainee Research Prize to attend this meeting.

3. Work from this grant has led to manuscript submission to International Journal of Radiaton Oncology, Biology, Physics, and is currently under review.

4. Work supported by this grant had led to significant preliminary data, which allowed Dong Kim to apply for the New Investigator Award from the DOD. Unfortunately, this grant was not funded, but received a favorable score (1.7).